JOURNAL OF OPTOELECTRONICS AND ADVANCED MATERIALS, Vol. 11, No. 3, March 2009, p. 243 - 250

SiO_2 thin films obtained from silica sols by thermal spraying

V. NIKOLIC, V. JOKANOVIĆ[a*], N. RADIĆ, B. GRBIĆ, B. JOKANOVIĆ[b], D. IZVONAR[c]
Institute of Chemistry, Technology and Metallurgy, Department of Catalysis, Njegoševa 12, 11000 Belgrade, Serbia
[a]Institute of Nuclear Sciences "Vinča", P.O. Box 522, 11001 Belgrade, Serbia, [b]Sol Carbon GmbH, Meintigen, Germany
[c]Faculty of ContemporaryArts, Kralja Petra 4, Belgrade, Serbia

The mechanism of the synthesis of silicon dioxide thin films on the surface of a stainless steel band substrate, by thermal spraying of a silica sol as a precursor was the subject of this work. The structural design of the hydro thermally obtained particles was defined as an organized structure of basic motives-silica tetrahedrons, over silica chains and finally sol particles, which were used as a well-defined precursor for the preparation of corresponding thin films. IR spectroscopy and TGA analysis were employed to define the structure of the silica tetrahedrons and the size of the silica chains in the sol particles. The thickness of the film and the dependence of the film morphology and structure on its surface and of its cross section were investigated. The mechanism of film formation and the differences on its appearance depending of the SiO_2 sol concentration was also investigated. The sizes of the particles were 50 – 250 nm, while the agglomerate sizes were mostly 250 nm in diameter and 1 – 2 μm in the length. The thicknesses of the films were 6.5 – 33 μm.

(Received February 9, 2009; accepted March 19, 2009)

Keywords: Thermal spray pyrolysis, Hydrothermal synthesis, Silica sol, Stainless steel tape, Nanostructured design

1. Introduction

Silicon dioxide films have been used in space technologies for oxidation protection of the surface of carbon-carbon and carbon- SiC composite materials. It is also used for the protection of magnetic ceramic materials, the properties of which depend on valence state of the constitutive ions, which is sensitive to changes in the partial pressure of oxygen [1]. Another application of thin SiO_2 films is as corrosion protective barrier for piezo-electrics [2]. They are also used in non-linear optics [3], electro-optics [4], and as a protective layer within systems that incorporate thermo-sensitive organic molecules [5]. Also, SiO_2 films are used as the active component of absorbents, chromatographic fillers, optical filters, and for the manufacture of integrated wave guiding optics components [6], etc.

They are often used also as a catalyst support in heterogeneous catalysis, because they can provide a high surface area substrate for the deposition of well dispersed catalytically active materials within the film of SiO_2 coatings. Ceramic or metallic monoliths structured as foam or straight parallel channels are suitable substrates for coating by SiO_2 films. In recent years, metallic monoliths have become increasingly popular due to their high thermal conductivity, low heat capacities, large thermal and mechanical shock resistance, high cell density and low pressure drop [7].

Thermal spray pyrolysis is one of the most promising methods for the deposition of thin films with a well-defined phase composition and chemical homogeneity. The principle advantage, besides its simplicity, results from the fact that each individual drop of an aerosol is itself a separate system, which possesses all the characteristics of the system as the whole, – its chemistry and phase composition [8– 17]. In addition to SP, there are numerous other methods for the deposition of thin films, such as the chemical vapor deposition (CVD) method assisted with different types of plasmas (microwave, radio frequency, laser induced and thermal plasma), reactive cathode vacuum arc deposition, deposition stimulated by electron-beam evaporation, reactive magnetron sputtering, electrophoretic deposition, ultrasonic spray pyrolysis and others [18– 26]. Although, some of these methods result in increased adhesion of the deposited films and greater smoothness (CVD deposition) compared to thermal spray pyrolysis deposited ones, SP still counts for one of the most convenient method of deposition on substrates of very diverse shapes and forms. The cost of the method is significantly lower and the method is applicable to various substrate/film systems, whereby the excellent chemical and phase homogeneity of the films is retained [25, 26].

Proper choice of SiO_2 precursors as nanomaterial follow by hydrothermal synthesis in the subsequent step of spray pyrolysis, enables precisely designed structures of silica particles to be obtained [27]. This approach to the synthesis clearly supports the elements of molecular and nanoengineering, which may have substantial importance in future investigations of self-assembled systems by the thermal spraying methods.

In this study, the spray pyrolysis method was used for the homogeneous wetting of stainless steel substrates with the droplets of a SiO_2 sol, with well-defined size distribution of SiO_2, followed by thermal treatment, which solidifies the deposit into a thin film. Also, a hydrothermal method for the synthesis of a SiO_2 sol, as one of the most

promising methods for the preparation of very preciously tailored precursors, was considered. The influence of the spray pyrolysis parameters on the thickness, morphology and roughness of the SiO2 films was investigated.

2. Experimental

2.1. Spray pyrolysis method

The spray pyrolysis apparatus for the synthesis of oxide coatings on tape of stainless steel has been presented in detail elsewhere [28].

Briefly, the apparatus consisted of a movable twin - fluid spray reactor. The precursor solution was introduced to the glass nozzle, diameter of 0.2 mm, at a flow adjustable using a peristaltic pump. Atomization of the liquid precursor was achieved by an air flow introduced to the nozzle with a controlled flow rate. The flow rate of the liquid precursor was maintained at 44 ml/h and the air flow rate for atomization of the liquid was 300 l/h. The whole spray was part of a self-made computer driven device which enabled nozzle movement at a chosen speed and direction. The employed distances between the nozzle and substrate (Stainless steel (SS) tape, Sandvik OC 404, thickness 35 μm) were 4 cm and 11 cm, creating a spraying spot on the substrate, of diameter 2.0 cm and 5.5 cm, respectively. A rectangular SS tape, external surface area of 30 cm^2 (3 x 10 cm) was used as the substrate. The nozzle movement was directed parallel to the longer rectangular side of the SS tape and after each pass, the nozzle pathway was shifted by 1 mm in the direction of the shorter rectangular side. The speed of the nozzle movement was 1 cm/s. The substrate temperature during the spraying was maintained by resistive heating. The applied voltage regulated the temperature of the SS tape but various temperature regimes simultaneously existed on the substrate surface during the spraying. Namely, resistive heating, without spraying, creates a relatively uniform temperature over the whole surface of the substrate. The periodic law motion of the spraying spot (ϕ-2.0 cm or 5.5 cm) over the surface significantly cooled down the corresponding area of the substrate due to the high air flow rate. When the spraying spot moved away from the targeted area, the temperature of substrate was quickly reestablished to its initial value. This situation was continuously repeated over the substrate during the spraying. The initial temperature of the substrate was 420 °C while at the center of the spraying spot, the temperature dropped to about 100 ° C. The nozzle speed (1 cm/s) provided a sufficient length of time, at least 15 s, for the deposited precursor drop to undergo several consecutive processes: solvent evaporation, precursor precipitation, drying, pyrolysis of precursors and film growing due to crystallization. This operating mode is similar to that of the conventional pulse spray pyrolysis method with a fixed nozzle [29-32].

The duration of the substrate spraying was varied in the range of 26 to 39 min. As precursors, a silica sol with a SiO_2 concentration in the range from 9 to 17 mass.% was used. In certain runs, poly(vinyl alcohol) was added to the precursor solution at a concentration of 0.2 wt.%.

2.2. Key preparation parameters

The SiO_2 coatings were deposited on one side of the stainless steel substrates. The content of deposited coatings was determined by the mass difference before and after the deposition of the layers. Key preparation parameters of the synthesized samples are presented in Table 1.

Table 1. Key preparation parameters of the synthesized samples

Nozzle to substrate distance (cm)	Spraying duration (min)	SiO_2 concentration in precursor solution (wt.%)	Initial temperature of substrate (°C)	Air flow rate (l/h)	Precursor solution flow rate (ml/h)
4	26	17	420	300	44
4	39	13.5	420	300	44
4	39	9*	420	300	44
11	39	1*	460	300	44

* Poly(vinyl alcohol) added

Keeping the nozzle to substrate distance at 4 cm and the flow rates of the precursor solution and air constant, the SiO_2 loadings were in accordance with the concentration of SiO_2 in the precursor solution and the duration of spraying. This enables the production of the desired SiO_2 content on the substrate and, consequently, the targeted film thickness. On addition of poly(vinyl alcohol), PVA, to the precursor solution, the content of SiO_2 was not affected. Bearing in mind the multiple passages of the nozzle over the substrate (nearly 4 times per min), a uniform coverage of the exposed substrate was obtained.

Increasing the nozzle distance from 4 to 11 cm produced a low SiO_2 content, indicating poor adhesion of the SiO_2 to the substrate, regardless of the presence of PVA. Also, for all samples, the calculations based on the SiO_2 content and the overall specific surface area showed that the deposited SiO_2 phase had a specific surface area of about 107 m^2/g.

2.3. Characterization methods

Both, the SiO_2 powder and the SiO_2 films on a stainless steel tape were subjected to detailed characterization.

The following characterization methods were used for the synthesized SiO_2 powder materials. Transmission electron microscopy, TEM, (JOEL JEM 2000 FX) and IR spectroscopy (PERKIN ELMER 983G) for phase analysis. Thermogravimetric and differential thermal analysis, TGA/DTA, (AMNICO) of the SiO_2 powder (obtained by drying the SiO_2 powder at 150 °C), to determine the structural motives of the SiO_2 sol particles, based on the determination of the water bound in them. The heating rates from room to the final temperature of 800 °C were 5 and 50 °C/min, respectively.

The morphology, size distribution, average size of the silicon dioxide particles, and substructure of the SiO_2 films deposited on a stainless steel substrate were determined by scanning electron microscopy, SEM, (JEOL: JKSM-5300). The samples for SEM were prepared by coating the powder with gold using the PVD method. The particle size was determined by applying the line intersection method on a scanning microphotograph with over 200 particles for each sample.

The specific surface area of the SiO_2 films was measured by nitrogen adsorption at – 196 °C using a self-made apparatus equipped with the TCD detector of a Varian Aerograph (model 920) gas chromatograph. The specific surface areas of the samples were calculated by the "one point" BET method. The apparatus was designed for a high degree of sensitivity and provided for measurement of a surface area as low as 0.1 m^2 in the sample cell. Before the measurements, the samples were treated at 450 °C in a helium flow for 2 h. Then, a gas mixture of 27 vol % nitrogen in helium (30 cm^3/min) was passed over the sample and sample cell was cooled by immersion in liquid nitrogen. The cooled sample adsorbed a certain amount of nitrogen from the gas stream and an adsorption equilibrium was established. When the liquid nitrogen bath was removed, the sample warmed and the adsorbed nitrogen was released, enriching the effluent, which was monitored by the TCD detector. When desorption was complete, a known volume of nitrogen (0.5 cm^3) was added to the nitrogen-helium stream. By comparing the desorption and calibration peaks, the volume of nitrogen adsorbed by the sample was calculated and the surface area of the sample was determined in a manner similar to that used in a standard volumetric BET method.

3. Results and discussion

3.1. Characterization of SiO_2 precursor

3.1.1. Infrared spectroscopy

Silica sol after drying: The IR spectrum of the silica sol dried at 150 °C exhibited bands at 3382 cm^{-1}, i.e., 3395 cm^{-1}, corresponding to the extended vibration of the silanol group (Si-OH) (Fig. 1). The twisting vibration of the OH^- group of molecular water is at 1579 cm^{-1} (usual literature value 1628 cm^{-1}). The band at 1325 cm^{-1} corresponds to the transversal and longitudinal asymmetric vibrations of siloxan rings-silica tetrahedrons, with dominant longitudinal vibration, while the bands at 1057 and 1030 cm^{-1} are corresponding to the transversal asymmetric Si-O-Si vibrations. Shifting of their wave number to slightly smaller values probably is caused by the movement of O atoms along the direction parallel to the Si-Si axis and distortion in adjacent Si-O bonds and the asymmetric transversal oscillations of corresponding cations [22-27,33].

The oscillation at 910 cm^{-1} with a small shoulder indicates an extended Si-OH vibration. The vibrations at 750 cm^{-1} and 416 cm^{-1}, related to the rocking vibration deformations in Si-O-Si chains, are shifted toward a slightly smaller wave numbers due to the couplings of transversal symmetric vibrations of O atoms along the bisection line of the Si-O-Si angle, with simultaneous movement of Si cations.

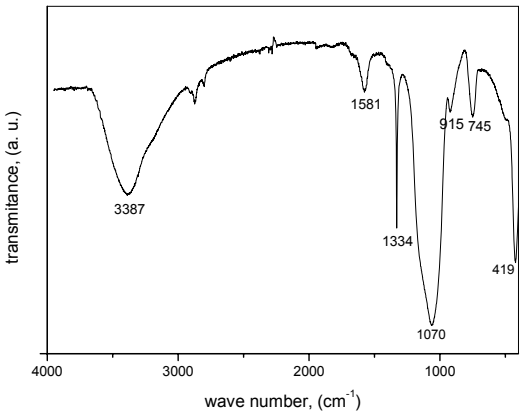

Fig.1. IR spectra for the sample of silica sol dried at 150 °C

3.1.2. Calculation of the basic structural unit of the silica sol over thermochemical analysis

By using TGA method from the mass loss of silica sol during of the dehodroxilation process as it is shown more preciously in ref 33 (see all needed details), the length of silica chains as a constructive subelements of silica sol particles and carriers of potential activity in the process of nucleation of CHA thin films from supersaturated SBF solution by using biomimetic method [34].was determined.

Briefly, the theoretical mass loss in the dehydroxylation process of silicon acid during the formation of a given structural unit is 37.5 %, involving 2 OH^- and 2 H^+ ions (the mass of H^+ is much lower than that of OH^- and may be neglected). This assumed that each silicate chain contains two OH^- groups, one per any chain end. In accordance to this, the calculated number of OH^-

groups, corresponding to mass loss of 3.02 % was 0.16 OH^- groups per one silicon acid chain.

In accordance with this assumption, the mass of the average length of the silica chains, M_{SiO2}, is expressed by:

$$n\,M_{Si} + (2n-1)\,M_O + 2\,M_{OH} = M_{SiO2}\,, \qquad (1)$$

where M_{Si}, M_O and $M_{OH,}$ are the atomic masses of Si, O and OH, respectively. Furthermore:

$$\frac{2M_{OH}}{nM_{Si} + (2n-1)M_O + 2M_{OH}} = u_{OH}\,. \qquad (2)$$

From more exact calculations, the results show that about 40 % of the chains have 16 assembled Si atoms and about 60 % have 20 assembled Si atoms.

Assuming a linear and extended chain, what is an unrealistic case, the length of the chain could be between 4.8 nm and 6.1 nm. Furthermore, the largest chain diameter (tetrahedron base) could be 0.14 nm (the length of the baseline). In accordance, the chain volume could be between 0.073 nm^3 and 0.092 nm^3.

Finally, assuming a more realistic case, i.e., spherical or spheroid chain forms, the SiO_2 chains could have diameters between 0.5 nm and 1 nm, depending on the form regularity (ellipsoid eccentricity). Such forms could be easily assembled in similar forms at the sol particle level (spherical shape, as was shown from TEM measurements).

3.1.3. Silica sol particles: transmission electron microscopy

The particle size of silica sol was determined using transmission electron microscopy.

The TEM microphotograph (Fig. 2.) shows that the sizes of the silica particles are between 5 and 10 nm, while their shape is mostly spherical, representing agglomerates of finer particles. At the particle edge, contours of smaller particles can be observed. The mean size of these small particles is 7.5 nm.

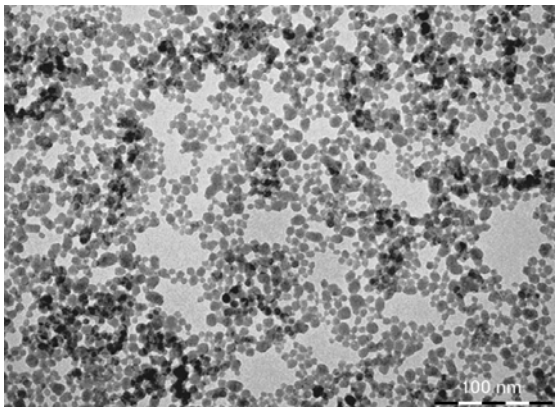

Fig.2. TEM micrograph of silica sol particles.

3.2. SiO_2 thin film characterization

Sample with a 17 wt % SiO_2 : The depth of the film measured by using the SEM method was about 33 μm (Fig 3a). The film consisted of very clearly distinguishable thinner layers, sub-layers (7 sub-layers), each with a thickness of about 5 μm.

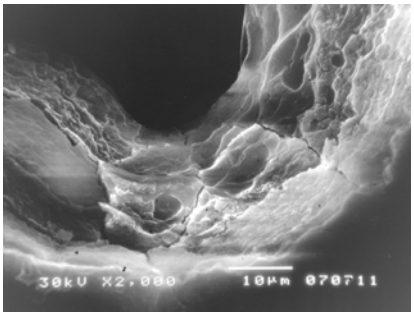

a

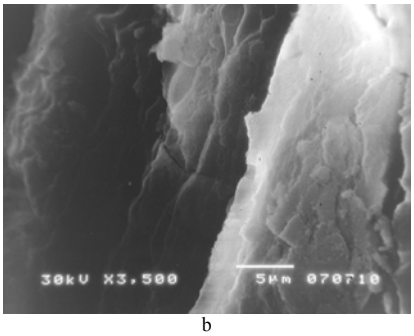

b

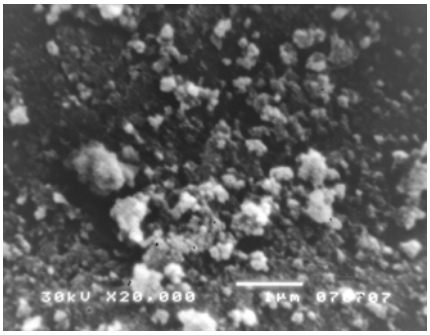

C

Fig.3. SEM micrographs of the surface of SiO_2/stainless steel for content of SiO_2 of 17 mass .%; a) Cross-sections and b) and c) typical appearance

The layers showed satisfactory homogeneity and clearly pronounced boundaries of their separation. They showed characteristic morphology: interconnected curvilinear hilly areas (Fig 3b). Certain cracks among the layers were noticed in some places (Fig 3a and 3b). In the other parts, the layers were clearly intergrown. The cracks and formed pores of the sizes between 1.5 and 2 μm among the layers were noticed. The strongly interconnected blocks inside of these layers consisting of particles of about 250 nm were also observed.

The non-homogeneity inside nearby layers and within the whole film is clearly visible in Fig. 3c. The maximal size of the agglomerates was close to 1 μm, while the single particles were about 50 – 100 nm (Fig. 3c). Areas of less dense packing, with a particle size of 1 – 2 μm, were noticed. Some of these building blocks were several micrometers in length. The single particles were mostly of spherical shape. They were preferentially present on the surface of the newly formed layers, because in these parts the time of their thermal treatment was probably insufficient for their intergrowth with the nearby, previously formed layers.

Sample with a 13.5 wt % SiO_2: In certain areas of the film surfaces, the presence of agglomerates of about 350 nm in size was evident. The smallest particles were between 50 – 90 nm in size (Fig. 4b).

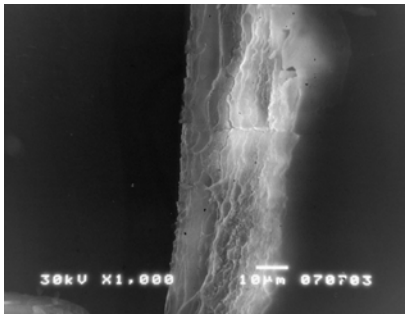

a

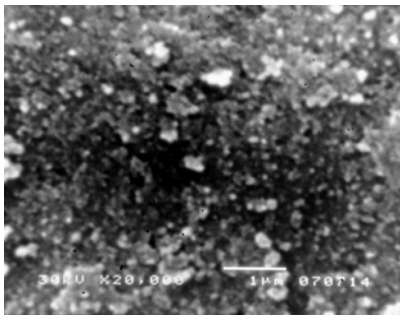

b

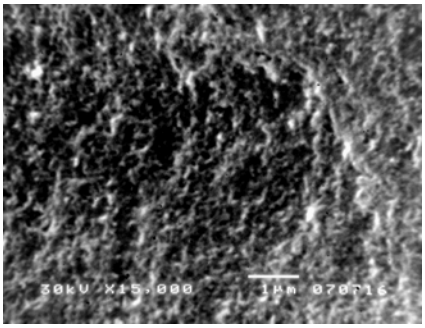

c

Fig.4. SEM micrographs of the surface of SiO_2/stainless steel for content of SiO_2 of 13.5 mas.%; a) Cross-sections and b) and c) typical appearance

They were mostly spherical and interconnected with monolithic ensembles of particles in the previously deposited layer. The film showed uniformly distributed pores, with the pore sizes in the range of the 100 – 150 nm (Fig. 4c). The total depth of the film was 22.5 nm (Fig. 4a). The film layers overlapped each other and they were not monolithic. The monolith structure of the film was pronounced only close to its surface.

The adhesion of the film with the substrate of the steel tape was not satisfactory in some places. This could have been caused by the specific surface morphology and the roughness of the tape and the concentration of the silica sol. A less homogeneous film substrate was visible in some places. Agglomerates of size 1 μm, with 50 – 100 nm particles in various levels of the film were observed. The particles in some places were joined into blocks of several μm in size. Canal pores, 250 nm in diameter and 1 – 2 μm long, were also noticed on the film surface and among the different film layers (Fig. 4b).

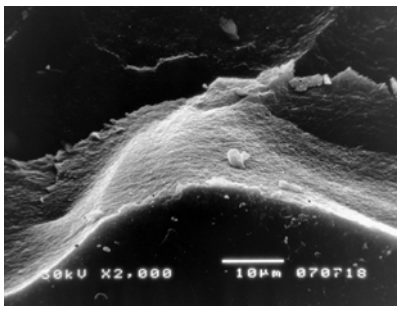

a

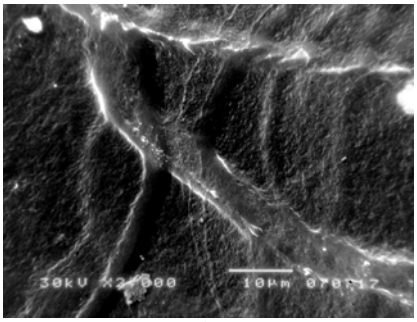

b

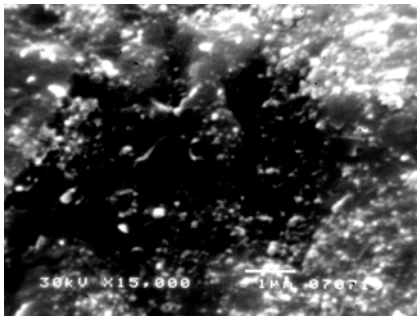

c

Fig. 5. SEM micrographs of the surface of SiO_2/stainless steel for content of SiO_2 of 9 mass.%; a) Cross-sections and b) and c) typical appearance

Sample with a 9 wt % SiO_2: The estimated thickness of the film was 15 μm (Fig. 5a). The film was

preferentially monolithic, consisting of several interconnected layers, with discrete pronounced boundaries.

The adhesion to the surface of the steel tape substrate was much better than in the cases of the 17 and 13.5 % deposited films. The deeper layers consisted of rows of smaller thickness layers. The boundaries among these layers were not clearly pronounced. The layers consisted of particles of about 100 nm in size. These particles made the rows built one on another from the bottom to the top of the film.

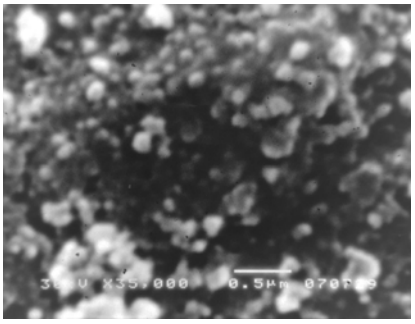

a

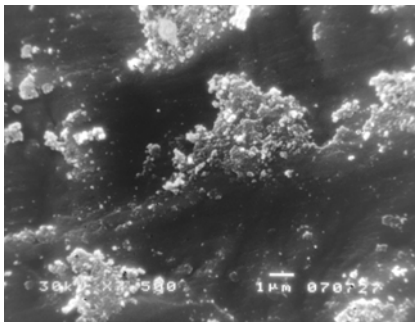

b

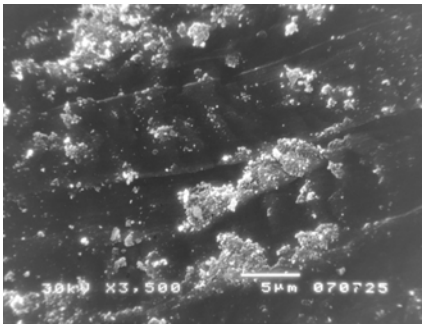

c

Fig.6. SEM micrographs of the surface of SiO_2/stainless steel for content of SiO_2 of 1 mass.%; a), b) and c) typical appearance

The cross section of the film, presented in Fig. 5a, showed a dense texture. In certain areas, strongly interconnected parts of these films were observed. Their depth was more than 2.5 μm and length more than 25 μm. They appeared as reinforced laps of the contact layers, causing their strong monolith intergrowth. Agglomerates of 1 μm size were observed. Inside of them, particles of 70 nm in size were observed. In a smaller amount, particles of 250 nm were also observed. The groups of the agglomerates and particles were not uniformly distributed. Zones of bigger building blocks with a thickness of 250 nm and a length of 4 μm were noticed in the spots. Particles sizes between 100 and 250 nm were observed on the film surface. They were not completely joined with the underlying layers. Therefore, in these spots, particles of the right sizes were visible.

Sample with a 1 wt.% SiO_2. The sizes of the particles on the surface of the film were between 50 and 70 nm (Fig. 6).

They formed mostly small agglomerates of sizes of 150 – 250 nm, while the largest agglomerates were about 500 nm. The boundaries between particles inside of these agglomerates were clearly visible.

The groups of the particles in contact with steel tape consisted of agglomerates of 3 – 4 μm in size. In some areas, the depth of the film was only 200 – 250 nm. The process of secondary nucleation was clearly present. Characteristic bridges between isolated islands on the steel substrate were seen. The areas with the most defects were occupied. Groups of particles of size between 70 and 100 nm were interconnected into agglomerates of 500 nm. These groups were mostly of irregular shape. Groups of 'grape fruit' shape, non-homogenously distributed, were observed. Smaller tapes in the direction of the tape rolling were also noticed. Their sizes were 10 – 15 μm in length and 2.5 – 5 μm in diameter. The mechanism of the secondary nucleation, which resulted in the mutual connection of neighboring isolated islands of particles into agglomerates, was evident.

Morphology of the substrate: A ribbed steel tape with its defect structure is shown in Fig. 7.

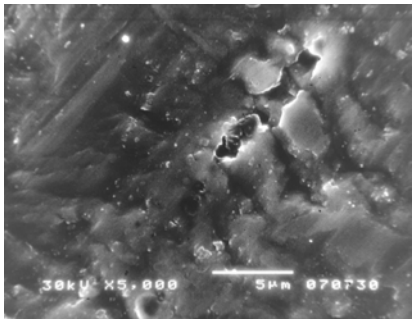

a

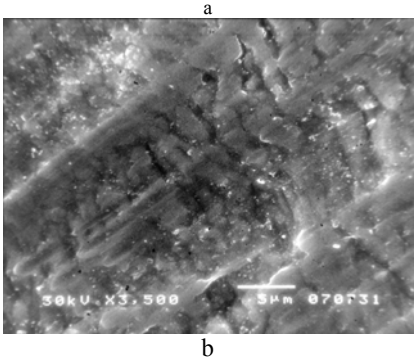

b

Fig.7. SEM micrographs of the stainless steel surface; a) and b) typical appearance

The typical appearance of 'fish scale' with the 'plates' ranging around 3 μm is visible. The direction of the tape rolling and the substrate porosity is also evident. The 'fish plates' visible in Fig. 10 were about 500 nm in diameter and 2.5 – 3.5 μm long. All these morphological features might have had an influence on the film deposition process and the adhesion characteristics of the films.

3.2.1. General remarks:

From the results of the SEM measurements, it is clear that the size of the single particles was between 50 and 100 nm in all the cases of deposition of the SiO_2 sol. From the corresponding reduction factor, it can be concluded that the sizes of the silica sol droplets were between 500 and 1000 nm. These droplets were probably formed during the secondary process of pyrolysis. The largest sizes of the particles were about 250 – 500 nm and the corresponding droplets sizes were 15 – 50 μm. This is the consequence of the bimodal droplet distribution, caused by the coalescence of droplets or by the typical size distribution of the droplets, in which some droplets are much bigger than others. The structure of the sol particles were pronounced even in the final phase of their solidification into film form, which was confirmed by the very high surface areas of the SiO_2 films (between 100 and 120 m^2/g), whereby the radius of the constitutive elements - particles were in the range 8 – 10 nm (that is, the diameter of the silica sol particles-TEM).

It seems that the described procedure could be very promising for the one-step production of multilayer coatings with a great variety of properties. Also, this procedure is prominent as the preparation method catalyst supports. The spray pyrolysis method permits the preparation of SiO_2 films with a relatively large thickness with a developed surface area, suitable as the substrate for the deposition of catalytically active materials.

3.2.2. IR spectroscopy of SiO_2 thin films

All bands observed in the dried sols are also visible in the thin film samples obtained by the spray pyrolysis, although some of the bands are slightly shifted. The band corresponding to the vibration of silanol groups is shifted from 3382 cm^{-1} to 3388 cm^{-1} and the band corresponding to the bending vibration of the OH^- group is shifted from 1597 to 1557 cm^{-1}. The intensities of the bands corresponding to OH^- vibrations are significantly reduced and at 1557 cm^{-1} almost disappears (Fig. 8). [35-37].

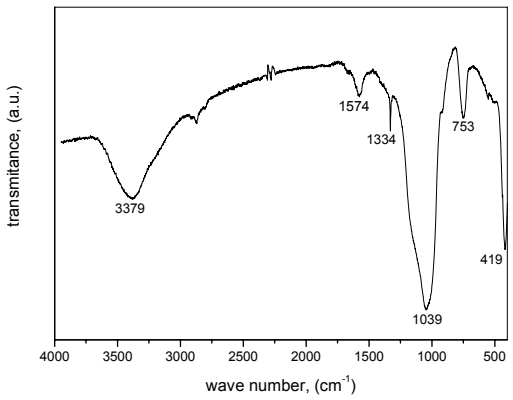

Fig. 8. The IR spectra of the silica film obtained by the spray pyrolysis process

4. Conclusions

The deposition of the SiO_2 thin film on a steel tape substrate was investigated for loadings of 17, 13.5, 9 and 1 mass %. The spray pyrolysis method enables the production of the desired SiO_2 content on a stainless steel substrate and, consequently, of the targeted SiO_2 film thickness.

The thickness of the film and the dependence of the film morphology and structure on its surface and through of its cross section revealed that the film thicknesses were between 6.5 and 33 μm for samples with a content of SiO_2 in the range 9 – 17 mass %, respectively.

The adhesion on the steel tape substrate was stronger for the concentration of the hydrothermally obtained silica sol of 9 mass.% than for 17 and 13.5 mass.%. This was because the particles and constitutive layers of this SiO_2 film were more densely packed than in the films obtained from silica sols of the others concentrations.

The sizes of the single particles in all films were between 50 and 100 nm. The biggest of them were 250 – 500 nm. The agglomerates sizes were in the range of the 1 – 2 μm. Only in some areas were blocks with sizes of the several micrometers observed.

The complete films for all SiO_2 concentrations were constituted from divided thinner layers, which were clearly visible in the SEM figures.

The high surface areas of the SiO_2 film measured by BET showed that all the SiO_2 particles consisted of very small SiO_2 sol particles of sizes below 10 nm, which was in agreement with the diameters of the SiO_2 sol particles obtained by TEM.

The structure motive, shape and size of the SiO_2 particles from the precursor solution were retained in the SiO_2 powder obtained by drying as well as in the SiO_2 films produced by spray pyrolysis.

References

[1] L. Borum, O. C. Wilson, Biomaterials **24,** 3681 **(**2003).
[2] A. Krozer, N. Stig-Arne, K. Bengt, J. Coll. Interf. Sci., **176,** 479 (1995).
[3] Q. Liu, B. Poumellec, X. Zhao, G. Girard, J.-E. Bourée, Kudlinski A., Martinelli G., J. NonCryst. Sol., **354**, (2008), 472-475.
[4] Okubo, T., Tsuchida, A., Tanahashi, T., Iwata, A., J.Coll. Interf. Sci., **207**, (1998),130-136
[5] Mohammad A. Optics Com. **271**, (2007), 457-461
[6] R.N. Thurston, J. Sound Vibr., **159**, (1992), 441-467
[7] P. Avila, M. Montes, E. E. Miro, Chem. Eng. J., **109**, 11–36 (2005)
[8] S.W. Kang, Y.S. Kim, J Korean Inst Met Mater **34** (1996), pp. 1375–1381.
[9] T. Damjanović, Chr. Argirusis, B. Jokanović, G. Borchardt, K. Moritz, E. Müller, R. Herbig, R. Weiss, J. Europ. Cer. Soc., **27**, (2007), 1299-1302
[10] W. H. Suh, K. S. Suslik, J. Am. Chem. Soc., **127**, (2005), 12007-12010.
[11] H. Sertchook, D. Avnir, Chem. Mater. **15**, (2003), 1690-1694
[12] D. Hreniak, E. Zych, L. Kepinski, W. Strek, J. Phys. Chem. Solids, **64**, (2003), 111-119.
[13] A. Lempicki, A. J. Wojtowich, C. Brecher, in: S. R. Rotman (Ed.), Wide-gap luminescent materials: Theory and applications, Kluwer, MA, 1996.
[14] R. Bertoncello, L. Milanese, R. Negro, L. Saragoni, S. Barison, J. Non-Cryst. Solids **324**, (2003), 73-78.
[15] Y. Fukada, P. S. Nicholson, J. Eur. Cer. Soc. **24** (2004) 17-23.
[16] D.W. Wojciechowska, J.K. Jeszka, P. Uznanski, C. Amiens, B. Chaudret and P. Lecante, Mater. Sci. Poland **22** (2004) (4), pp. 407–413
[17] O. D. Velev, T. A. Jede, R. F. Lobo, A. M. Lenhoff, Porous Silica via Colloidal Crystallization Nature, **389**, (1997), 447-448
[18] J. Kraitchman, J. Appl. Phys. **38,** 4323 (1967).
[19] Z.X. Zhao, R.Q. Cui, F.Y. Meng, B.C. Zhao, H.C. Yu Z.B. Zhou, Mat. Lett., **58**, 3963 (2004).
[20] M Takeda., M Ichimura., H Yamaguchi., Y Sakairi, K Kimura, J.Sol. St. Chem., **154**, 141 (2000).
[21] P. Bulkin, N. Bertrand., B. Drévillon., J. C. Rostaing, F. Delmott., M. C Hugon, B Agius, Thin Solid Films, **308-309**, 63 (1997).
[22] J. Mueller, Thin Sol. Fil., **401**, 84 (2001).
[23] C. S McCormick., C. E Weber., J. R Abelson., S. M Gates., Appl. Phys. Lett. **70**(2), 226 (1997).
[24] Y. Castro., A. Duran., R. Moreno, B. Ferrari, Adv.Mater. **14**, 505 (2002).
[25] V. Jokanović, A. M. Spasić, D Uskoković, Journal of Colloid and Interface Science, **278**, 342 (2004).
[26] V. Jokanović, D. Uskoković, JIM, **46**(2), 228 (2005).
[27] V. Jokanović, M.D. Dramićanin, Ž. Andrić, B. Jokanović, Z. Nedić, A. M. Spasic, Journal of Alloys and Compounds, **453** , 253 (2008).
[28] T. Novaković, N. Radić, B. Grbić, T. Marinova, P. Stefanov, D. Stoychev, Catal. Comm. **9**(6), 1111 (2008).
[29] J. D. Desai, Sun-Ki Min, Kwang-Deog Jung, Oh-Shim Joo, Appl. Surf. Sci. **253,** 1781 (2006).
[30] W. Sheng-Yue, L. Zu-Hong, Mater. Chem. Phys. **78,** 542 (2003).
[31] R. V. Todorovska, S. T. Groudeva-Zotova, D. S. Todorovsky, , Mater. Lett. **56,** 770 (2002).
[32] B. A. Reguig, A. Khelil, L. Cattin, M. Morsli, J.C. Bernède, Appl. Surf. Sci. **253,** 4330 (2007).
[33] V. Jokanović, B. Jokanović, J. Optoelectron. Adv. Mater. **10**, 2684 (2008).
[34] B. Colovic, V. Jokanovic, B. Markovic-Todorovic, Z. Markovic, J. Optoelectron. Adv. Mater. **11**, 70 (2008),
[35] A. van Blaaden, A. Vrij, Langmuir, **8**, 2921 (1992).
[36] F. Geotti-Bianchini, M. Preo, M. Guglielmi, C. G. Pantano, J. Non-Cryst. Solids **321,** 110 (2003).
[37] P. Innocenzi, J. Non-Cryst. Solids **316**, 309 (2003).

*Corresponding author: vukomanj@beotel.net;
vukoman@vin.bg.ac.yu ,